© 2014 Westinghouse Electric Company LLC. All Rights Reserved

PHYSOR 2014 – The Role of Reactor Physics Toward a Sustainable Future
The Westin Miyako, Kyoto, Japan, September 28 – October 3, 2014, on CD-ROM (2014)

AP1000® PWR REACTOR PHYSICS ANALYSIS WITH VERA-CS AND KENO-VI - PART I: ZERO POWER PHYSICS TESTS

F. Franceschini
Westinghouse Electric Co. LLC,
Cranberry Township, Pennsylvania, USA
francef@westinghouse.com

A. T. Godfrey, J. C. Gehin
Oak Ridge National Laboratory
godfreyat@ornl.gov

ABSTRACT

Westinghouse has applied the Core Simulator of the Virtual Environment for Reactor Applications, VERA-CS, under development by the Consortium for Advanced Simulation of LWRs (CASL) to the core physics analysis of the **AP1000**® PWR. The **AP1000** PWR features an advanced first core with radial and axial heterogeneities, including enrichment zoning, multiple burnable absorbers, and a combination of light and heavy control banks to enable the MSHIM™ advanced operational strategy. These advanced features make application of VERA-CS to the **AP1000** PWR first core especially relevant to qualify VERA performance. A companion paper at this conference describes the power distribution analysis of the **AP1000** PWR with VERA-CS and the KENO Monte-Carlo code. This paper describes the results obtained for the startup physics tests simulations of the **AP1000** PWR first core (critical boron, rod worth and reactivity coefficients), supporting the excellent numerical agreement reported in the companion paper for the power distribution.

Key Words: **AP1000 PWR, VERA, CASL, KENO**

1 INTRODUCTION

The **AP1000** PWR features a low-leakage 18-month cycle advanced first core, with five fuel regions, intra-assembly enrichment zoning, and a combination of burnable absorbers: the Westinghouse Integral Fuel Burnable Absorber (IFBA) a ZrB_2 coating on the pellet surface, and the Wet Annular Burnable Absorber (WABA), an insert employed at selected guide thimble locations [1]. Light tungsten banks and standard Ag-In-Cd banks are employed for MSHIM™ core control strategy, an advanced operational strategy that provides robust core reactivity and axial power distribution control with minimal changes to the soluble boron concentration during both normal operation and power maneuvers[2],[3]. These advanced features make application of the Virtual Environment for Reactor Applications (VERA) for this analysis especially relevant to qualify its performance.

An extensive set of simulations has been performed throughout this activity. The results present-

AP1000® and MSHIM™ are trademarks or registered trademarks of Westinghouse Electric Company LLC in the United States and may be registered in other countries throughout the world. All rights reserved. Unauthorized use is strictly prohibited.

CASL-U-2015-0005-000

ed are focused on Hot Zero Power (HZP) simulations, where given the fresh fuel and uniform temperature conditions it is possible to establish Monte-Carlo Continuous Energy reference solutions for validation of the VERA results, in lieu of measurements. In particular, the All-Rods-Out (ARO) Critical Boron Concentration (CBC), reactivity coefficients and the Control Rod Worth have been calculated, similarly to Nuclear Design calculations that support Zero Power Physics Tests (ZPPTs). A companion paper at this conference describes the results obtained for the power distribution analysis.[4]

The SP_5 VERA solver with P_3 scattering in 23 energy groups and on-the-fly pin-homogenized cross-sections generated from a 252-group ENDF BVII.0 SCALE library has been used [5],[6]. The Monte-Carlo simulations have been performed using a developmental version of the KENO Monte-Carlo code [10]. The VERA simulations have been performed on the Westinghouse computer cluster, while the KENO simulations have been performed on the INL Fission computer cluster.

2 AP1000 PWR FIRST CORE DESIGN

The **AP1000** PWR first core, which is being deployed in the units under construction, is described in detail in Ref. [1]. The core and fuel characteristics are summarized in Table 1.

The core features five fresh fuel regions (Table 2), arranged with the core loading pattern shown in Figure 1. The ^{235}U enrichments span the range from natural U to 4.8 w/o ^{235}U. The placement of natural U (Region 1) on some of the peripheral assemblies helps achieving a low leakage design which improves fuel cycle economics. The checkerboard of lower and higher enriched fuel (Region 2 and 4 respectively) in the inner part of the core mimics the conditions of subsequent reloads, containing fresh and burned fuel assemblies. The position of the highest enriched assemblies (Region 5) slightly inboard from the periphery favors radial power distribution control over the cycle.

Regions 1 to 3 feature uniform ^{235}U enrichment, radially. Regions 4 and 5 feature radial enrichment zoning in the middle part of the stack, with rods at three ^{235}U enrichments. The enrichment zoning for these regions, with the lowest enrichment pins located on the assembly periphery, aims at reducing the interface effects with the neighboring, low enrichment, fuel assemblies. The intra assembly loading patterns for Regions 4 and 5 are shown in Figure 2.

Two types of burnable absorbers are used in the **AP1000** PWR first core: the Westinghouse Integral Fuel Burnable Absorber (IFBA), a ZrB_2 coating on the pellet of selected fuel rods, and the Wet Annular Burnable Absorber (WABA), an annular insert containing an Al_2O_3-B_4C mixture, with water flowing in the inner part of the rod. These burnable absorbers are used in Regions 4 and 5, with the assembly loading patterns showed in Figure 2. The burnable absorber disposition in the core is shown in Figure 1.

The fuel axial stack is depicted in Figure 3. Region 1 and 2 fuel assemblies do not feature axial blankets given the lower enrichment and the absence of burnable absorbers. Top and bottom 8-in blankets are employed in Regions 3 to 5. The blankets have lower enrichment with respect to the remainder central part of the fuel stack and consist of solid pellets in non IFBA fuel rods, and annular pellets in IFBA rods. The inner void of the IFBA annular blankets provides additional room for expansion of the He released from (n, alpha) reactions in ^{10}B.

CASL-U-2015-0005-000

Table 1 AP1000 PWR Core Fuel Characteristics

Active fuel height (in.), cold	168
Assembly Number Rod pitch (in.) Fuel rods per assembly Fuel rods Cladding OD, Gap, Thickness (in) Guide Thimble above dashpot (in) a Gude Thimble at dashpot (in) Instrument guide thimbles (in.)	17 x 17 square array 157 0.496 264 0.374, 0.0065, 0.0225 0.442 ID x 0.482 OD 0.397 ID x 0.482 OD 0.442 ID x 0.482 OD
Dashpot length (in, from bottom of active fuel)	23
Number of grids in the active fuel Mixing Vane (MV) Intermediate Flow Mixing (IFM)	12 8 4
Cladding and active fuel grid material	ZIRLO™
Discrete Burnable Absorber Number Material External and Internal Tube material Inner/Outer Tube OD (in) B-10 Content (mg/in) Absorber Length	Wet Annular Burnable Absorber (WA- 592 Al2O3-B4C Zircaloy 0.267/0.381 15.32 Variable
Integral Fuel Burnable Absorber Material Number B-10 Content (mg/in) Absorber Length	IFBA ZrB2 coating 5632 1.96 152
Reactivity Control Cluster Assemblies	53 Standard + 16 Gray
Neutron absorbers	Standard: Ag-In-Cd Gray: Tungsten + Alloy 718
Diameter (in.)	Standard: 0.341 Gray: Tungsten 0.197 / Alloy 718 0.310
Cladding thickness (in.)	Standard: 0.0185 Gray: 0.0225
Cladding OD (in) Cladding material Number of absorber rods per cluster	0.381 Stainless Steel 24

ZIRLO™ is a trademark or registered trademark of Westinghouse Electric Company LLC in the United States and may be registered in other countries throughout the world. All rights reserved. Unauthorized use is strictly prohibited.

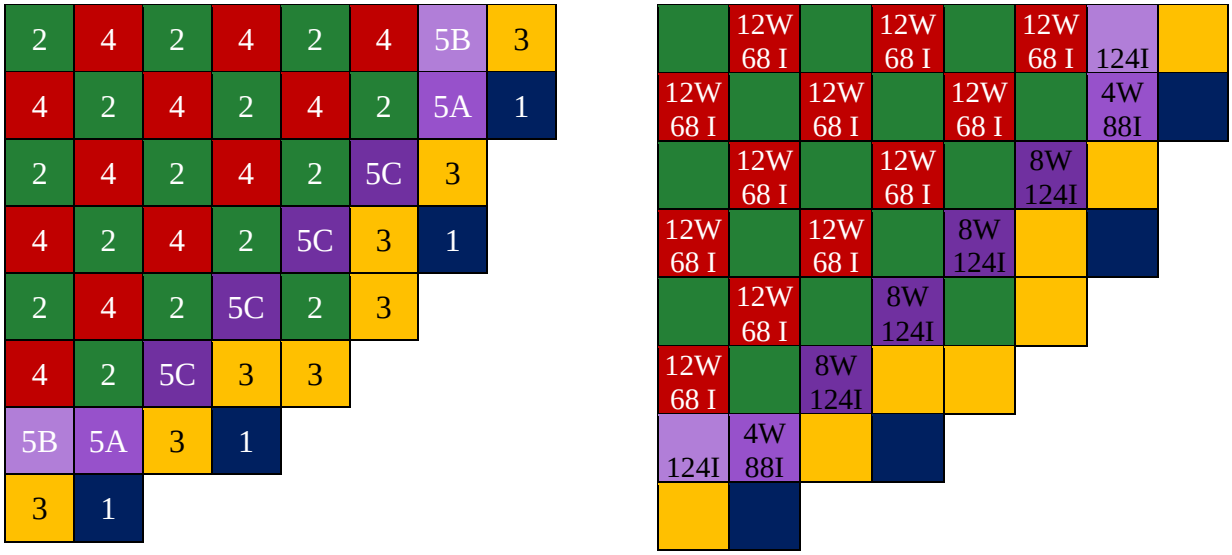

Figure 1 Core Loading Map for the **AP1000** PWR First Core, quarter core geometry (region identifier shown on the left map; number of burnable absorber rods shown on the right map, "W": WABA; "I": IFBA)

Table 2 Fuel Summary Characteristics by Regio**n**

Region Identifier	Fraction of Total	U235 Midzone	U235 Blanket	IFBA Rods	WABA Rods
1	0.10	0.740	Absent	0	0
2	0.31	1.580	Absent	0	0
3	0.18	3.200	1.580	0	0
4	0.23	3.776	3.200	68	8L+4S
5A	0.05	4.376	3.200	88	4I
5B	0.03	4.376	3.200	124	0
5C	0.10	4.376	3.200	124	8I

IT	M	M	SW	M	M	LW	M	LI
M	HI	H	M	H	H	M	M	L
M	H	HI	M	HI	HI	M	M	LI
SW	M	M	GT	M	M	GT	MI	L
M	H	HI	M	M	M	M	M	LI
M	H	HI	M	M	LW	M	M	L
LW	M	M	GT	M	M	M	M	LI
M	M	M	MI	M	M	M	MI	L
LI	L	LI	L	LI	L	LI	L	LI

L	32	3.40	No BA
LI	32	3.40	IFBA
M	140	3.80	No BA
MI	12	3.80	IFBA
H	24	4.20	No BA
HI	24	4.20	IFBA
SW	4		WABA
LW	8		WABA

IT	M	M	GT	M	M	GT	MI	LI
M	H	H	M	H	H	M	M	LI
M	H	H	M	HI	HI	M	MI	LI
GT	M	M	GT	M	M	GT	MI	LI
M	H	HI	M	M	M	M	M	LI
M	H	HI	M	M	W	M	M	LI
GT	M	M	GT	M	M	M	M	L
MI	M	MI	MI	M	M	M	M	LI
LI	LI	LI	LI	LI	LI	L	LI	L

L	12	4.00	No BA
LI	52	4.00	IFBA
M	132	4.40	No BA
MI	20	4.40	IFBA
H	32	4.80	No BA
HI	16	4.80	IFBA
W	4		WABA

IT	M	M	W	M	M	GT	MI	LI
M	HI	H	M	H	HI	M	M	LI
M	H	H	M	HI	HI	M	MI	LI
W	M	M	GT	M	M	GT	MI	LI
M	H	HI	M	M	M	MI	M	LI
M	HI	HI	M	M	W	M	M	LI
GT	M	M	GT	MI	M	M	M	LI
MI	M	MI	MI	M	M	M	MI	LI
LI	LI	LI	LI	LI	LI	LI	LI	LI

LI	64	4.00	IFBA
M	120	4.40	No BA
MI	32	4.40	IFBA
H	20	4.80	No BA
HI	28	4.80	IFBA
W	8		WABA

Figure 2 Assembly loading pattern for Region 4 (top), 5A (middle) and 5C (bottom) at the core axial mid-plane. Region 5B loading pattern is same as 5A except for the absence of WABA inserts.

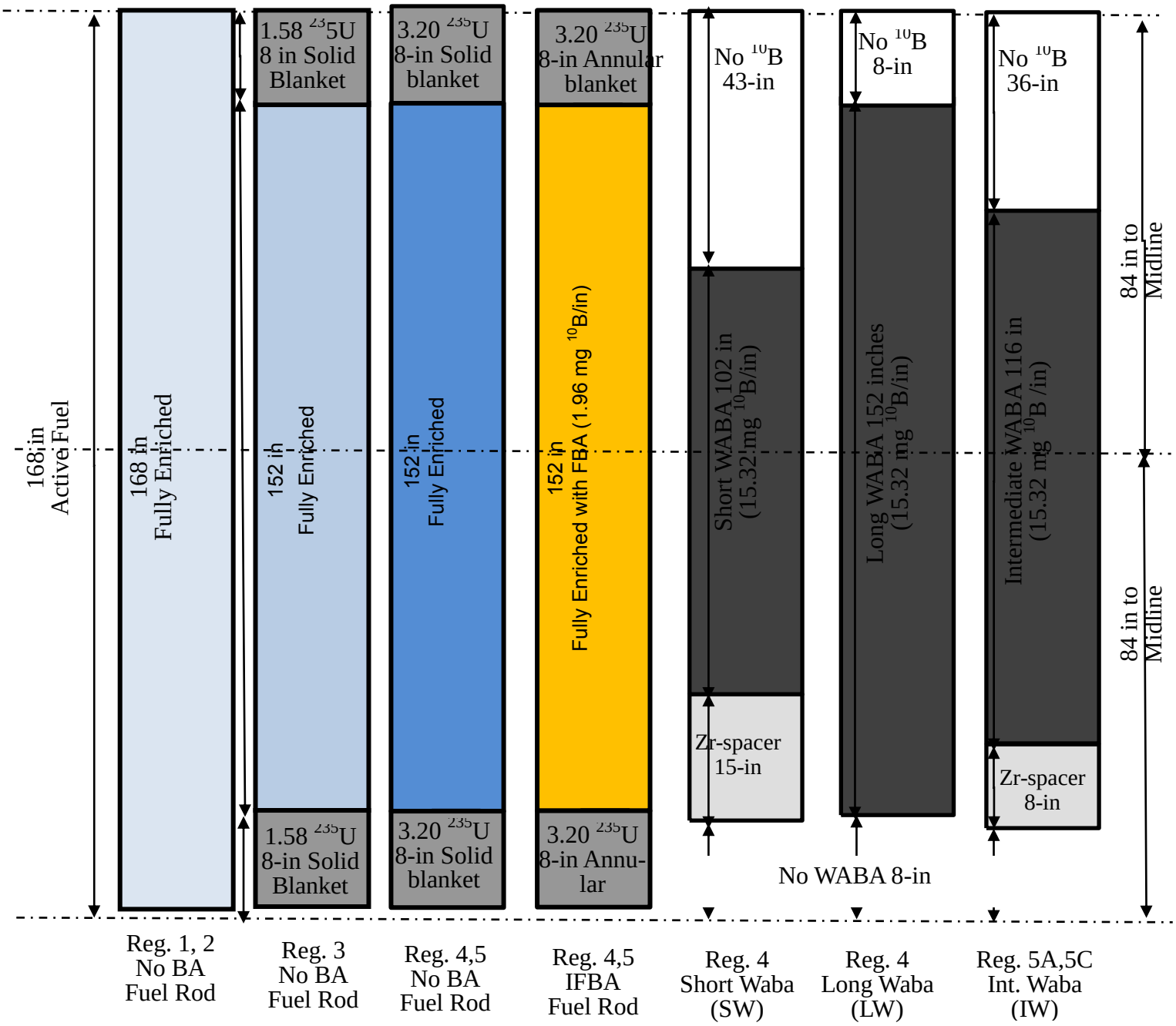

Figure 3 Axial configuration for fuel rods and WABA inserts for each region

CASL-U-2015-0005-000

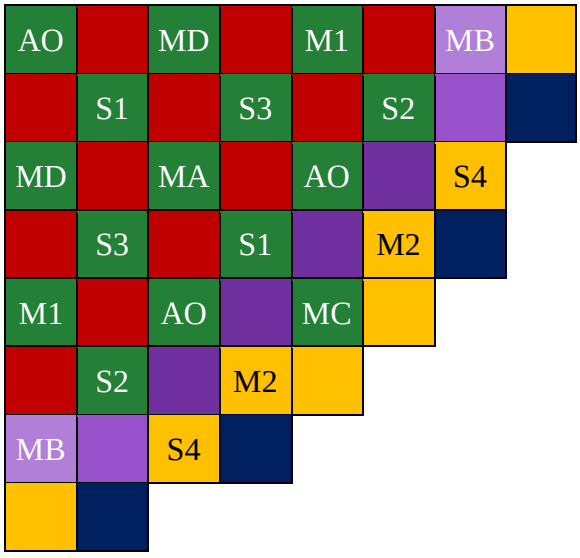

Figure 4 Control Bank core configuration

Table 3 Control Bank Functionality

Bank ID	Functionality	Type	# of RCCAs
MA	MSHIM	Gray	4
MB	MSHIM	Gray	4
MC	MSHIM	Gray	4
MD	MSHIM	Gray	4
M1	MSHIM	Black	4
M2	MSHIM	Black	8
AO	AO Control	Black	9
S1	Shut-down	Black	8
S2	Shut-down	Black	8
S3	Shut-down	Black	8
S4	Shut-down	Black	8

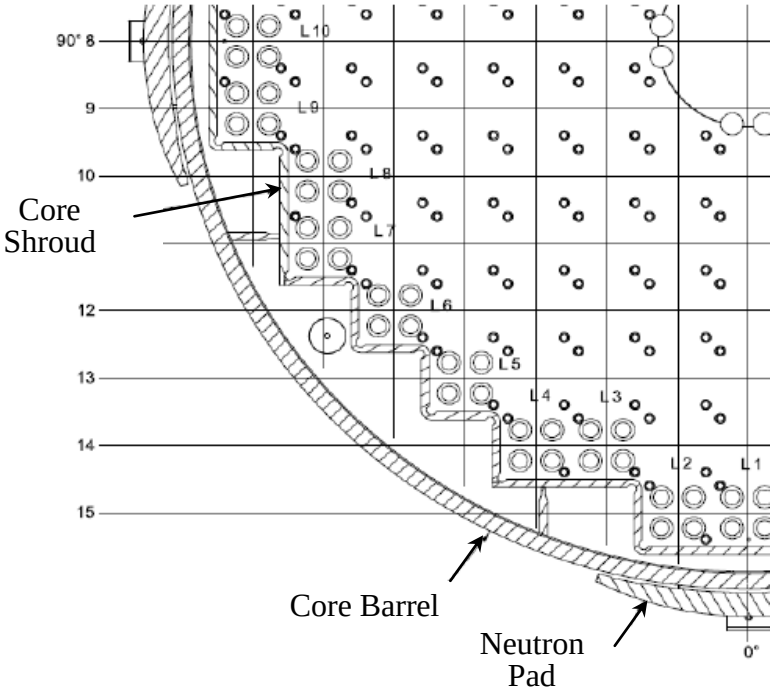

Figure 5 Reflector Structure– Radial View

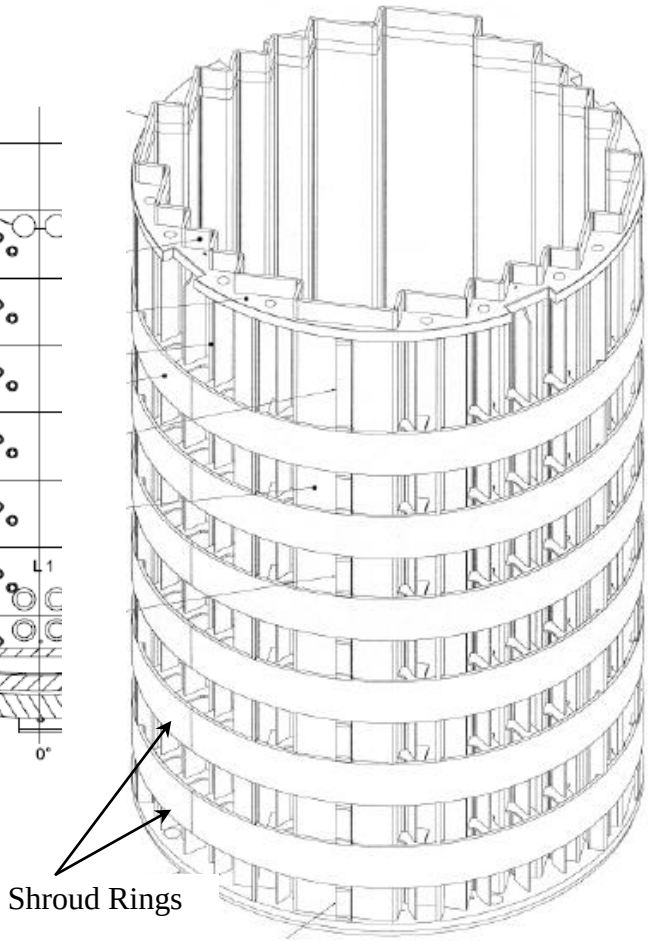

Figure 6 Core Shroud – Isometric View

The WABA inserts have three axial configurations (see Figure 3): the short and long WABA, used in Region 4, and the intermediate WABA, used in Region 5, featuring respectively a 102 in, 152 in and 116 in ^{10}B bearing central region. This poisoned region is offset downward with respect to the fuel axial midplane to counterbalance the effect of the Axial Offset (AO) Control Bank, which is typically inserted at the top of the core. An unpoisoned upper plenum zone is featured at the top of the WABA, while a Zr spacer is employed at the bottom of Region 4 short WABA and Region 5 intermediate WABA.

There are 12 ZIRLO™ grids in the **AP1000** PWR core active fuel, 8 Mixing Vane (MV) grids, with a height of 2.25 in, and 4 shorter Intermediate Flow Mixing (IFM) grids with a height of 0.66 in. Two Inconel grids are present at the top and bottom of the stack; one protective Inconel grid is placed after the bottom nozzle.

The core arrangement and material specifications for the control rod banks are shown in Figure 4 and Table 3. A combination of low worth (or gray) control cluster assemblies and standard (or black) control cluster assemblies is employed to implement the MSHIM operation and control strategy. The MSHIM strategy provides robust reactivity and axial power distribution control with minimal changes to the soluble boron concentration in the reactor coolant system during both normal and power maneuvering scenarios[2],[3]. This strategy necessitates an increased presence of control clusters in the reactor core during operation. Out of a total of 69 reactivity control cluster assemblies (RCCAs), 16 gray RCCAs plus 12 black RCCAs ("M" banks in Figure 4 and Table 3) are used for MSHIM operation and 9 black RCCA ("AO" bank) are used for axial offset control. The remaining 32 black RCCAs are dedicated shut-down ("SD") banks. The control rod poison used for the black banks is Ag-In-Cd while tungsten within an Inconel liner is used for the gray banks.

The structure surrounding the reactor core is shown in Figure 5 and Figure 6. The main component is a core shroud, which has a baffle with several axial rings and connecting structure. A cylindrical barrel with four neutron pads is also present outside the shroud. The thickness of the baffle and the rings is ~ 1-in, with a ~2-in thick barrel. The material is stainless steel 304.

3 AP1000 PWR CORE MODELING

3.1 VERA-CS

The SP_N solver with on-the-fly cell-homogenized cross sections generated using the SCALE module XSProc ([5],[6]) has been used for VERA-CS. Namely, SP_5 with P_3 scattering and 23 energy group cross sections data collapsed from the 252 energy group ENDF/ B-VII.0-based SCALE library using 1D discrete ordinate transport pin cell calculations have been employed.

XSProc performs resonance self-shielding with full range Bondarenko factors using the BONAMI module of the SCALE system and employing either the narrow resonance approximation or the intermediate resonance approximation. A wide variety of options are provided for different lattices and cell geometries through the use of Dancoff approximations. For uniform fuel lattices, Dancoff factors are automatically generated from the user-input geometry and material descriptions. The fine energy group structure of the resonance self-shielding calculation is then collapsed to a coarse group structure through a one-dimensional (1D) discrete-ordinates transport

CASL-U-2015-0005-000

calculation internal to XSProc. In addition a spatial homogenization is employed for pin cell cross sections also using the flux results from the 1D transport solution. The homogenized cross sections from XSProc are then used for the full-core SP_N transport calculation.

The SP_N method ([7]-[9]) is a low-order space-angle approximation of the Boltzmann equation. It is computationally advantageous because the matrix representing the transport operator can be explicitly formed, which opens many possibilities for parallel decomposition, preconditioning, and solvers. Even though SP_N does not converge to the true transport solution as the SP_N expansion is increased, it has been widely used and shown to be a significant improvement over diffusion theory for reactor problems. The implementation of SP_N in VERA-CS provides a low-order transport option to perform calculations on industry-size clusters while yielding adequate accuracy for ZPPT analysis, as shown here and in [12].

3.2 KENO-VI

The Monte Carlo criticality code KENO-VI ([10]) with parallel transport capabilities and using continuous energy (CE) energy treatment ([11]) has been used to obtain reference numerical solutions. The KENO simulations rely on an ENDF/B-VII.0 CE cross section library generated by the AMPX code system ([12]) at the HZP temperature of 565 K.

KENO-VI has been successfully compared against the Monte Carlo code MCNP5 ([14]) for lattice physics problems. KENO has also been successfully benchmarked against start-up measurements from the Watts Bar Unit 1ZPPT. [12]

The KENO-VI version used for this work is a development version to be released in SCALE 6.2 (Beta 2) that takes advantage of several new features, including parallelization of the particle transport and improvements in the CE data and methods.

3.3 Modeling Approach

VERA-CS models are set up through a common ASCII input, which is converted by a pre-processor to the specific input required by the lower-level codes (neutronics, thermal-hydraulic etc.) to set-up and execute the simulation. In this specific case, the steps below are performed:

1. Process ASCII input file with problem specification, converted into XML format
2. Convert input specification into arguments for XSProc
3. Generate a geometric representation of the reactor
4. Build and partition a discrete mesh representation of the reactor geometry
5. Broadcast XSProc geometry to each processor domain
6. Run XSProc to generate pin-cell homogenized macroscopic cross sections
7. Map the cross sections to VERA-CS computational mesh cells
8. Run the SP_N solver to calculate scalar fluxes
9. Integrate scalar fluxes with fission reaction rate data to calculate power distribution

CASL-U-2015-0005-000

10. Output results

The VERA input file allows detailed modeling of the **AP1000** PWR core features in a compact input file.

The KENO model for the **AP1000** PWR core has been produced using the SCALE Generalized Geometry Package, which permits construction of detailed PWR models by combining geometric shapes such as cylinders and cuboids, or any volume that can be constructed with quadratic equations. The model relies on quadrant symmetry to decrease computer resources. Reflective boundaries are used for the lines of symmetry, while vacuum boundaries are applied outside of the core radial and axial reflector.

Most core features are modeled explicitly, in both VERA and KENO. Regions above and below the fuel rods are treated as homogenized regions. In particular:

- The fuel rod stack, including plenum and end plugs, is represented explicitly. The end plug geometry is modeled as a cylinder, and is similar for fuel rods, WABA rods and control rods. The plenum spring is modeled as a shell of equivalent inner and outer radius and mass in KENO. The plenum springs is smeared in the plenum region in VERA.
- WABA, control rods, end plugs, and plenum regions below the top nozzle are modeled explicitly. The presence of inserts at and above the top nozzle is ignored. Control rods are included in the model up to the upper nozzle when fully withdrawn, which results in the rod tips being located in the fuel rod upper plenum region.
- Thimble plugs are included in the upper regions of the guide tubes which do not contain control or WABA rodlets. The plugs are modeled as solid cylinders with equivalent length to the actual plug.
- Guide tubes and instrument tubes are assumed to extend from the bottom nozzle to the top nozzle. The dashpot region of the guide tubes is modeled explicitly.
- Spacer, mixing, and protective grids are represented semi-explicitly in KENO, by uniformly distributing the grid mass in volume boxes of equivalent total mass, placed on the periphery of each cell. In VERA the grids are uniformly smeared in the coolant. The axial locations of the spacer grids are modeled according to [1]. The mass of the spacer sleeves is included as part of the grid mass.
- The top and bottom nozzles of each assembly, and the upper and lower core plates, are homogenized.
- In KENO, the core baffle and rings, barrel, neutron pads and vessel are modeled explicitly. The interconnecting structure of the shroud has been neglected. Due to current limitations in VERA, only the baffle and surrounding water could be modeled while the remaining structure (rings, barrel, neutron pads and vessel) has been neglected.

CASL-U-2015-0005-000

The KENO representation of the **AP1000** PWR start-up core is given in Figure 8. Radially, the model extends up to the reactor vessel, including the major structural materials outside of the core (e.g. shroud, neutron pad and barrel). Axially, the model extends from the bottom core plate to the top core plate.

3.4 Simulations Performed

The simulations reported in this paper refer to HZP ZPPTs, and namely consists of 3D core eigenvalue simulations at all-rods-out (ARO) conditions and with each individual bank completely inserted for rod worth prediction. Boron worth calculations have also been performed and the results have been used in the prediction of the HZP critical boron concentration for the **AP1000** PWR first core start-up. KENO simulations relying on various reflector models have been used to predict the reactivity impact of the simplified model assumed in VERA-CS vs. the KENO reflector model, which is a closer approximation of the actual **AP1000** PWR reflector. This allowed the determination of a reactivity bias to apply to the VERA results to improve the consistency in the comparison with KENO.

3.5 Computational Resources

VERA-CS simulations have been executed at Westinghouse on a parallel-computation system with 576 cores distributed on 48 nodes with a total memory of 96 GB/node (8 GB/core).

3D core eigenvalue VERA calculations have been performed employing a 2x2 radial mesh per pin with 73 axial meshes, resulting in 6 million computational cells. In 23 energy groups, with 3 degrees of freedom per space-energy location for the SP5, the resulting total number of degrees of freedom is over 400 million with > 32 billion nonzero entries in the matrix representing the SP5 operator. The resulting wall-time was ~1.5 hours on 320 cores, 48 core-hours, for state-point calculation with a memory usage of ~2.5 TB. The runtime breaks down in ~10% for cross section calculation by XSProc, ~30% for setup operations such as matrix and preconditioner construction, and ~60% for the SPN solver flux calculation.

Table 4 Summary Parameters for KENO Core Simulations

Parameter	Eigenvalue Only
Total # Particles	5 billion
# Particles / Generation	5 million
# Generations	1,000
# Skipped Generations	250
# Cores	180
Memory / Core	10.7 GB
Runtime	28 hours
Eigenvalue Uncertainty	< ± 1.5 pcm

The KENO calculations have been performed on the INL Fission computer cluster, with the main parameters summarized in Table 4. Five billion particles per case have been run, with five million particles per generation, 750 active generations and 250 initial generations skipped. The resulting eigenvalue statistical uncertainty is less than 2 pcm, which is adequate for global reactivity prediction (e.g., all-rods-out and rod worth eigenvalue calculations). These KENO simulations were executed in parallel, on 180 cores, with a wall-time of 28 hours and ~ 5,000 core-hours per state-point calculation, and a total memory usage of ~ 2TB.

4 RESULTS

The HZP ARO eigenvalue, rod worth and differential boron worth for the **AP1000** PWR first core predicted by VERA-CS and KENO are given in Table 5 and Table 7.

Except for the boron worth, all the simulations have been performed at the soluble boron concentration of 1321 ppm, consistent with the conditions reported in [1]. The boron worth calculations have been performed perturbing the soluble boron concentration by 25 ppm. The ARO critical boron concentration prediction from VERA-CS and KENO has been inferred based on the boron worth prediction and the eigenvalue calculated at 1321 ppm by each code.

The KENO results have been obtained using the 3D quarter-core model illustrated in Figure 8. The VERA-CS core model is consistent with the KENO model, except for the reflector region. Namely, a one-inch baffle stainless steel reflector surrounded by water has been employed in VERA-CS, while the KENO reflector model includes also the shroud rings, neutron pads and barrel.

A KENO calculation with the VERA reflector model shows that the reactivity bias from the difference between the VERA reflector and the explicit reflector models is -10 pcm, or worth ~ -1 ppm of soluble boron, at BOC. This bias has been applied to the VERA ARO results. Given its small magnitude, and the little impact of the different reflector models on neutron flux distribution except for the outermost core assembly locations, it is acceptable to use the simplified reflector model adopted in VERA-CS for the ZPPT calculations performed.

Using the above models, and applying the ~ -10 pcm correction to the VERA ARO eigenvalue results to account for the limitations in the reflector model, the difference in the ARO eigenvalue prediction between VERA and KENO is only ~ 30 pcm. The boron worth prediction between KENO and VERA is virtually identical at ~ 9.5 pcm/ppm.

It should be noted that cold dimensions and cold material specifications have been used in both KENO and VERA-CS simulations. While this ensures internal consistency in the comparison of the results from VERA and KENO, for realistic prediction of the HZP ARO CBC the effect of thermal expansion from cold to operating conditions should be accounted. The impact of thermal expansion has been calculated using the Westinghouse in-house core physics package ([15],[16]), which results in a ~ 120 pcm reduction in the eigenvalue prediction. In addition, the presence of instrumentation in selected instrumentation tubes has been separately accounted for using KENO, and resulting in a ~30 pcm reduction in the core eigenvalue.

CASL-U-2015-0005-000

Applying the above combined biases of ~ -150 pcm to the cold un-instrumented core eigenvalue reported in Table 5, and using the respective codes boron worth prediction, leads to a predicted start-up ARO CBC of 1313 ppm and 1310 ppm respectively for KENO and VERA-CS. This is the best estimate HZP ARO CBC from KENO and VERA for comparison to the measurements as the **AP1000** reactors will come on-line. It should be remarked that a 3 ppm difference in 3D core reactivity prediction from VERA and KENO is virtually a perfect agreement.

The temperature reactivity coefficients calculated with KENO and VERA are reported in Table 6. These coefficients have been generated perturbing each of the associated parameter (e.g. moderator temperature, density and fuel temperature), fitting the results using quadratic fits (moderator density variations) or linear fits (fuel and moderator temperature variations), and then adding up the various reactivity components. [17] The results indicate overall good agreement between VERA and KENO, with the VERA prediction being more negative than KENO. The Doppler Temperature Coefficient, DTC, is within -0.2 pcm/F. The Moderator Temperature Coefficient, MTC, differs by ~-0.4 pcm/F. An analysis of the reactivity components of the MTC shows that the difference in the predicted value is due primarily to the difference in the Moderator Density Coefficient. The discrepancies in the DTC and MTC predictions add up, resulting in a ~0.6 pcm/F more negative ITC in VERA compared to KENO.

Table 5 HZP Reactivity Results

	KENO	**VERA**	**VERA-KENO**
k_{eff} cold dimensions, 1321 ppm	1.00066 +/- 1 pcm	1.00033	-33 pcm +/- 1 pcm
Boron Worth pcm/ppm	-9.6	-9.4	+0.2
Startup critical boron hot dimensions, instrumented	**1313**	**1310**	**-3 ppm**

Table 6 Temperature Reactivity Coefficients

	KENO	**VERA**	**VERA-KENO**
Doppler Temperature Coefficient (DTC) pcm/F	-1.54	-1.72	-0.18
Moderator Temperature Coefficient (MTC) pcm/F	-1.12	-1.50	-0.38
Isothermal Temperature Coefficient (ITC) pcm/F	-2.66	-3.22	-0.56

Note: KENO temperature coefficient uncertainties estimated to be <0.1 pcm/F

The control rod worth results from VERA-CS and KENO are reported in Table 7, with differ-

CASL-U-2015-0005-000

ences depicted in Figure 7. The rod worth prediction from VERA-CS is also in excellent agreement with KENO, for all eleven control banks of the **AP1000** PWR. The resulting Root Mean Square (RMS) delta rod worth for VERA vs. KENO is 4 pcm, 0.8% as percentage of the rod worth. The maximum rod worth difference is 9 pcm, 2.1% in terms of percentage of the rod worth.

There is no apparent bias in the prediction from bank material (e.g. gray tungsten or black Ag-In-Cd) or bank location (internal or periphery of the core). Note that none of the outermost core assemblies, whose power prediction in VERA vs. KENO is slightly impacted by the difference in the reflector model implemented, have control rods.

Table 7 Control Bank Worth Results

		KENO	**VERA-CS**	
Bank	**Material**	**Worth (pcm)**	**ΔWorth (pcm)**	**ΔWorth (%)**
MA	Tungsten	258	-1	-0.5
MB	Tungsten	217	-5	-2.1
MC	Tungsten	188	-2	-1.1
MD	Tungsten	234	0	0.0
M1	Ag-In-Cd	651	-4	-0.6
M2	Ag-In-Cd	887	3	0.4
AO	Ag-In-Cd	1635	-4	-0.3
S1	Ag-In-Cd	1079	0	0.0
S2	Ag-In-Cd	1096	-9	-0.8
S3	Ag-In-Cd	1124	0	0.0
S4	Ag-In-Cd	580	-3	-0.4
		RMS	**4**	**0.8**
		Max	**9**	**2.1**

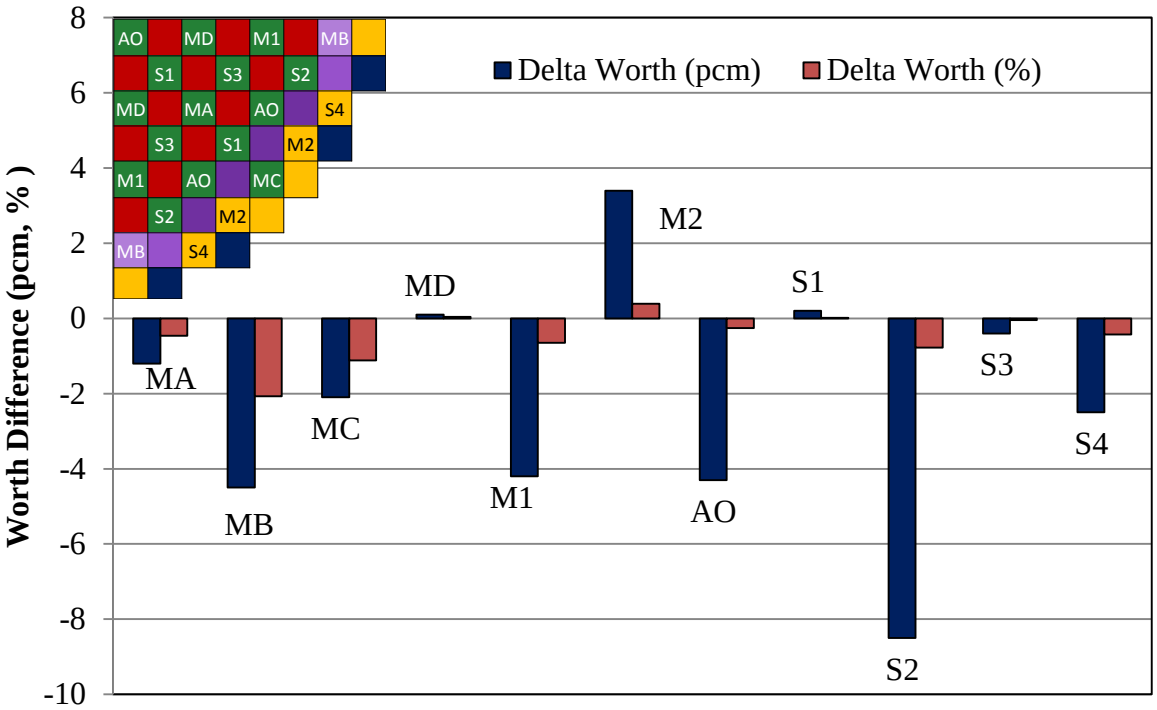

Figure 7 Delta in bank worth (in pcm and %) for VERA vs. KENO

5. CONCLUSIONS

Simulations of the zero power physics tests for the **AP1000** PWR first core have been performed using the CASL core simulator, VERA-CS, with the SP_N solver. In particular, the SP_5 solver with P_3 scattering and 23 energy group cross sections data collapsed from the 252 energy group ENDF/ B-VII.0-based SCALE library have been used. On-the-fly 1D discrete ordinate transport pin cell calculations have been used for the cross-section data collapsing.

The Monte Carlo criticality code KENO-VI with parallel transport capabilities and CE treatment has been used to obtain reference numerical solutions. The KENO simulations rely on an ENDF/B-VII.0 CE cross section library generated by the AMPX code system at the HZP temperature of 565 K.

The VERA simulations have been performed on the Westinghouse compute clusters. The wall-time for 3D core static eigenvalue calculations is ~1.5 hours on 320 cores, 48 core-hours, for state-point calculation with a memory usage of ~2.5 TB. The KENO calculations have been performed on the INL Fission computer cluster and executed in parallel on 180 cores, with a wall-time of 28 hours and ~ 5,000 core- hours per state-point calculation, with ~2 TB total memory.

VERA has shown excellent agreement with KENO for the simulations performed for this advanced core design, featuring radial and axial heterogeneities, IFBA and WABA burnable absorbers, enrichments from natural U to 4.8 w/o ^{235}U, and a combination of light tungsten control banks and heavy, Ag-In-Cd control banks to perform the MSHIM operational strategy..

In particular, the **AP1000** PWR HZP critical boron concentration predicted by VERA for the

CASL-U-2015-0005-000

start-up core is within 3 ppm of the KENO prediction. The difference in boron worth is 0.2 pcm/ppm. The DTC, MTC and ITC are respectively within 0.2, 0.4 and 0.6 pcm/F.

The RMS in the delta rod worth prediction is 4 pcm, with a maximum difference of 9 pcm, across the eleven control banks of the **AP1000** PWR. There is no apparent bias in the prediction with respect to bank material (e.g. gray tungsten or black Ag-In-Cd) or bank location (internal or periphery of the core).

The results of the ZPPT simulations from VERA are consistent with Westinghouse predictions using in-house core physics tools and licensed methods. This reinforces the confidence in the Westinghouse prediction for the start-up tests, as several **AP1000** units will soon begin operation.

ACKNOWLEDGMENTS

The authors would like to acknowledge the following individuals for their contribution to this work: Jeff Secker, Dave Salazar, Joel Kulesza, Greg Fischer, Larry Hampshire, Joseph Walsh (Westinghouse), Roscoe Bartlett, Mark Baird, Tom Evans, Kursat Bekar, Cihangir Celik (ORNL), Ben Collins, Aaron Graham (UM).

This research was partially supported by the Consortium for Advanced Simulation of Light Water Reactors (www.casl.gov), an Energy Innovation Hub (http://www.energy.gov/hubs) for Modeling and Simulation of Nuclear Reactors under U.S. Department of Energy Contract No. DE-AC05-00OR22725.

This research used resources of the Oak Ridge Leadership Computing Facility at the Oak Ridge National Laboratory, which is supported by the Office of Science of the U.S. Department of Energy under Contract No. DE-AC05-00OR22725. This research also used resources of the INL High Performance Computing (HPC) Facility at the Idaho National Laboratory.

REFERENCES

[1] M. Hone et al., AP1000 Core Reference Report, Westinghouse Electric Company, March 2012 WCAP-17524-NP

[2] T. Morita, et al., "Application of MSHIM Core Control Strategy for Westinghouse **AP1000** Nuclear Power Plant", GENES4/ANP2003, September 2003.

[3] K. Drudy, etc., Robustness of the MSHIM Operation and Control Strategy in the **AP1000** Design, 17th International Conference on Nuclear Engineering (ICONE 17), July 12-16, 2009, Brussels, Belgium

[4] F. Franceschini, et al., "**AP1000** PWR Reactor Physics Analysis with VERA-CS and KENO-VI – Part II: Power Distribution", PHYSOR 2014, Kyoto, Japan, September 28 – October 3, 2014

[5] T.M. Evans et al., 2010. Denovo: A New Three-Dimensional Parallel Discrete Ordinates Code in SCALE. Nuclear Technology, 171, pp.171–200.

[6] SCALE: A Comprehensive Modeling and Simulation Suite for Nuclear Safety Analysis and Design, ORNL/TM-2005/39, Version 6.1, June 2011. Available from Radiation Safety Information Computational Center at Oak Ridge National Laboratory as CCC-785.

[7] E. M. Gelbard, Applications of spherical harmonics method to reactor problems, Tech. Rep. WAPD-BT-20, Bettis Atomic Power Laboratory, 1960.

CASL-U-2015-0005-000

[8] E. W. Larsen, J. Morel, and J. McGhee, Asymptotic derivation of the simplified PN equations, Proc. ANS Topical Meeting, Mathematical Methods and Supercomputing in Nuclear Applications, 1 (1993), pp. 718-730.

[9] R. G. McClarren, Theoretical aspects of the simplified PN equations, Transport Theor. Stat. Phys., 39 (2011), pp. 73-109.

[10] D.F. Hollenbach, L.M. Petrie, and N.F. Landers, "KENO-VI: A General Quadratic Version of the KENO Program," Vol. II, Sect. F17 of SCALE: A Modular Code System for Performing Standardized Computer Analysis for Licensing Evaluation, NUREG/CR-0200, Rev. 7 (ORNL/NUREG/CR/CSD-2R7), 3 vols., April 2004. Available from the Radiation Safety Information Computational Center at Oak Ridge National Laboratory as CCC-545.

[11] B.T. Reardon et al., "Enhancements in Continuous-Energy Monte Carlo Capabilities for SCALE 6.2", PHYSOR 2014, Kyoto, Japan, September 28 – October 3, 2014.

[12] J.C. Gehin et al., "Watts Bar Unit 1 Cycle Zero Power Physics Tests Analysis with VERA-CS", PHYSOR 2014, Kyoto, Japan, September 28 – October 3, 2014.

[13] M.E. Dunn and N.M. Greene, "AMPX-2000: A Cross section Processing System for Generating Nuclear Data for Criticality Safety Applications," Trans. Am. Nucl. Soc. 86, 118–119 (2002).

[14] A.T. Godfrey, et al. "Analysis of Two-Dimensional Lattice Physics Verification Problems with MPACT", Dec. 21 2013, CASL-U-2012-0172-000

[15] L. Mayhue, R. Milanova, H. Huria, B. Zhang, E. Müller, F. Franceschini, M. Ouisloumen, P. Forslund Guimaraes, "Qualification of the NEXUS/ANC Nuclear Design System for PWR Analyses", PHYSOR-2008, Interlaken, Switzerland, September, 2008

[16] M. Ouisloumen et al.,"Qualification of the Two-Dimensional Transport Code PARAGON', WCAP-16045-NP-A, August, 2004.

[17] A. T. Godfrey et al., "Simulation of Watts Bar Unit 1 Initial Startup Tests with Continuous Energy Monte Carlo Methods", PHYSOR 2014, Kyoto, Japan, September 28 – October 3, 2014

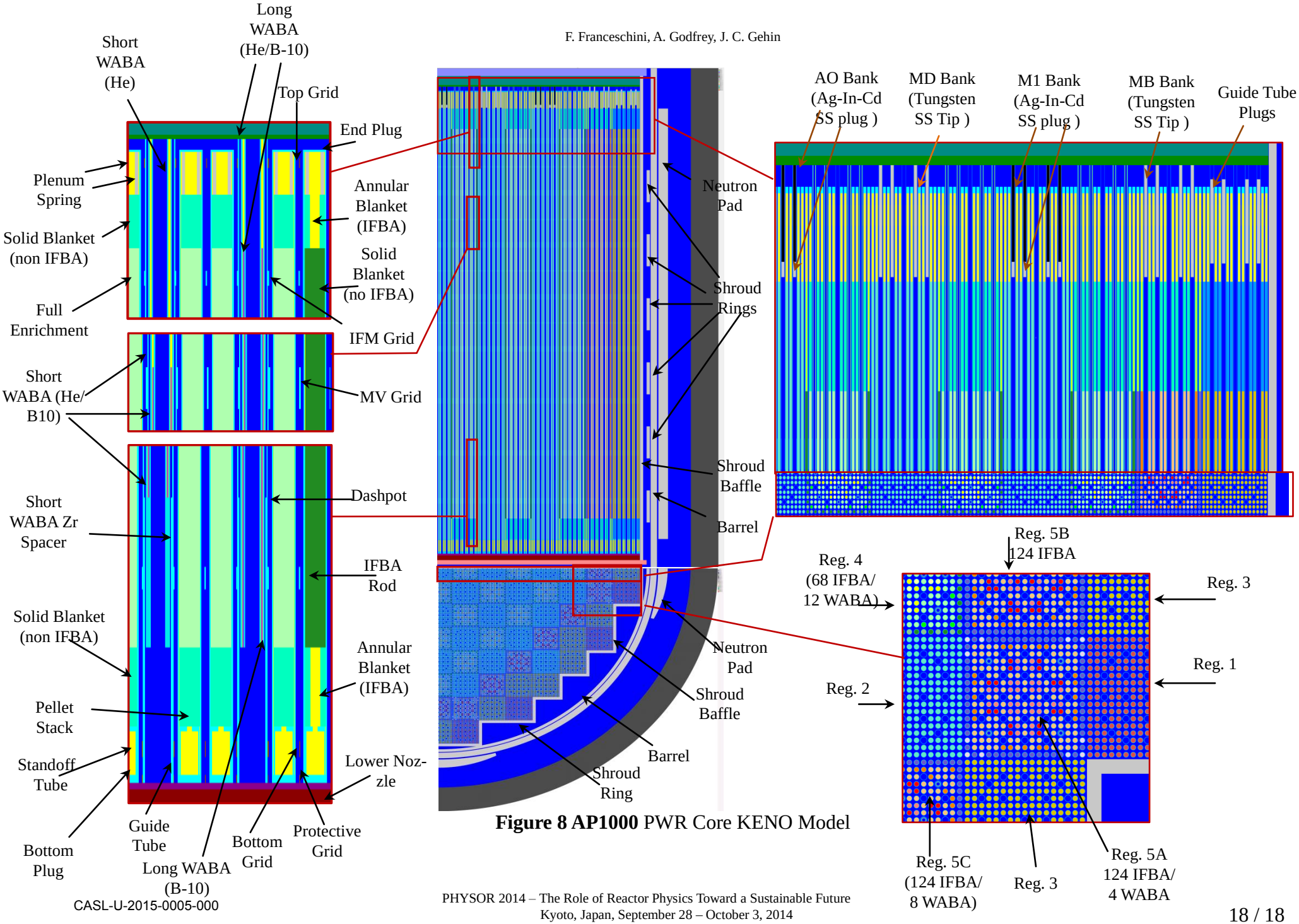

Figure 8 AP1000 PWR Core KENO Model